EPJ Web of Conferences **136**, 03010 (2017) DOI: 10.1051/epjconf/201713603010
*RICAP16*

# The Fermi-GBM Gamma-Ray Burst Catalogs: The First Six Years

E. Bissaldi[1,2,a], P. N. Bhat[3], and H.-F. Yu[4,5] for the Fermi-GBM Team

[1] *Dipartimento Interateneo di Fisica, Università e Politecnico di Bari, Bari, Italy*
[2] *INFN – Sezione di Bari, Bari, Italy*
[3] *CSPAR, University of Alabama in Huntsville, Hunstville, AL, USA*
[4] *Max Planck Institute for Extraterrestrial Physics, Garching, Germany*
[5] *Excellence Cluster Universe, Technical University of Munich, Munich, Germany*

**Abstract.** Since its launch in 2008, the Fermi Gamma-ray Burst Monitor (GBM) has triggered and located on average approximately two gamma-ray bursts (GRBs) every three days. Here we present the main results from the latest two catalogs provided by the Fermi-GBM science team, namely the third GBM GRB catalog [1] and the first GBM time-resolved spectral catalog [2]. The intention of the GBM GRB catalog is to provide information to the community on the most important observables of the GBM detected bursts. It comprises 1405 triggers identified as GRBs. For each one, location and main characteristics of the prompt emission, the duration, the peak flux and the fluence are derived. The GBM time-resolved spectral catalog presents high-quality time-resolved spectral analysis with high temporal and spectral resolution of the brightest bursts observed by Fermi GBM in a shorter period than the former catalog, namely four years. It comprises 1491 spectra from 81 bursts. Distributions of parameters, statistics of the parameter populations, parameter-parameter and parameter-uncertainty correlations, and their exact values are obtained.

## 1 The third GBM trigger catalog

From July 12$^{\text{th}}$, 2008 to July 11$^{\text{th}}$, 2014, GBM triggered on 3350 transient events. The left panel of Figure 1 shows the quarterly statistics over the aforementioned period, highlighting different sources with different colors. The total number of detected GRBs is 1404. From this number we can derive the six year average GRB rates, namely $(0.662 \pm 0.018)$ day$^{-1}$ or $(242 \pm 7)$ yr$^{-1}$. The GRB sky distribution in celestial coordinates is also shown in Figure 1. There are 1176 long GRBs ($T_{90} > 2$ s, black dots) and 228 short GRBs (blue asterisks). The isotropic distribution of long and short GRB arrival directions is evident. The lower fraction of GBM short GRBs (20.7%) compared to the one measured by BATSE (24%) is due to an excess of long events detected by GBM's longer timescale trigger algorithms.

### 1.1 The GRB catalog analysis – Main steps

**1) Burst localization** The distribution of systematic uncertainties in GBM positions is well represented (68% c.l.) by a Gaussian of standard deviation 3.7$^{\text{o}}$ with a non-Gaussian tail that contains

[a] e-mail: elisabetta.bissaldi@ba.infn.it

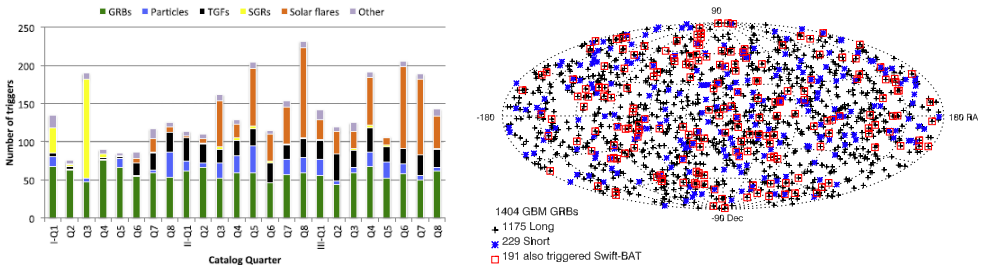


**Figure 1.** On the *left*: Quarterly trigger statistics over the first six years of the GBM mission. The different types of events triggering GBM are classified as shown at the top. On the *right*: Sky distribution of GBM-triggered GRBs during the first six years in celestial coordinates (RA and Dec). Crosses indicate long GRBs and asterisks indicate short GRBs. Also shown are the GBM GRBs simultaneously detected by Swift (red squares).

about 10% of GBM-detected GRBs and extends to approximately $14^{o}$ [3]. Moreover, probability maps are produced for every burst through convolution of the statistical uncertainty with the best current model for the systematic errors. The maps reflect the occasional noncircular shape of the statistical uncertainty region as well as its area.

**2) Detector Response Matrix (DRM) production** DRMs are generated using the General Response Simulation System [4] and are routinely delivered to the Fermi Science Support Center[1].

**3) GRB Duration, Peak Flux and Fluence computation** GRB $T_{50}$ and $T_{90}$ durations are computed through an automatic batch fit routine implemented within the spectroscopy software package RMFIT[2]. They represent the intervals between the times where the burst has reached 25%/5% and 75%/95% of its maximum fluence in the 50–300 keV energy range. Fluences are computed in two energy ranges, namely 50–300 keV and 10–1000 keV. Peak fluxes in the same energy ranges are given for three timescales (64, 256, and 1024 ms).

[1] `http://heasarc.gsfc.nasa.gov/FTP/fermi/data/gbm/bursts`
[2] `http://fermi.gsfc.nasa.gov/ssc/data/analysis/user/`

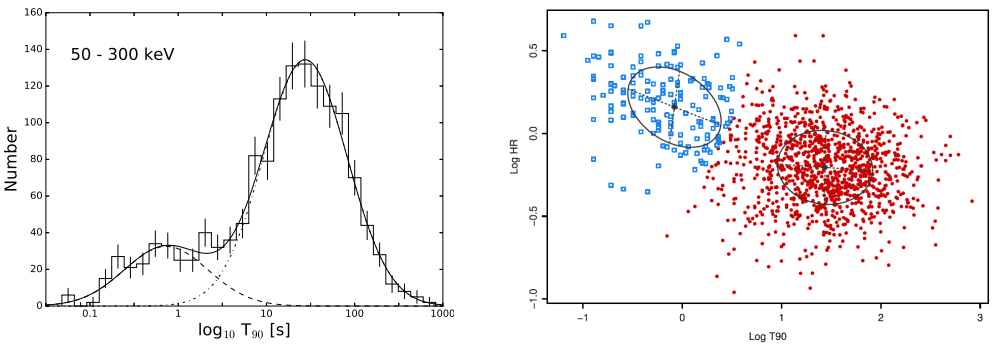


**Figure 2.** On the *left*: Distribution of GRB $T_{90}$ durations in the 50–300 keV energy range. Also, shown separately are the lognormal fits to long and short GRBs. On the *right*: Classification based on the hardness–duration diagram. Colors indicate their group membership (red: on average short/hard, blue: on average long/soft). Ellipses show the best-fitting multivariate Gaussian models.

### 1.2 The GRB catalog – main results

The left panel of Figure 2 shows the distributions of GBM durations. This is consistent with a bimodal distribution and it was verified by various independent analyses, namely trough (1) a model-based clustering method with lognormal model components [5]; (2) Monte Carlo simulations; and (3) a Bayesian Dirichlet mixture model [6]. The median $T_{90}$ durations are 26.62 s and 0.58 s for long and short bursts, respectively. The right panel of Figure 2 shows the hardness–duration diagram. It is consistent with two clusters: the short/hard group and the long/soft group. This was verified by independent analysis as was done for the duration distribution.

## 2 The first GBM time-resolved spectral catalog

Since the time-resolved spectral analysis requires bright bursts with sufficiently high signal-to-noise spectra, we applied following selection criteria to the bursts detected by GBM in the first four years (954 GRBs): energy fluence $f > 4 \times 10^{-5}$ erg cm$^{-2}$ and/or peak photon flux $F_p > 20$ ph s$^{-1}$cm$^{-2}$ (in either 64, 256, or 1024 ms), both in the 0.01–1 MeV energy range. Moreover, we required the presence of at least five time bins in the light curves when binned with signal-to-noise ratio = 30. 81 bursts satisfy these criteria (with only 1 short GRB 120323A). In the end, we obtained 1802 time-resolved time bins and spectra, which were analyzed with RMFIT considering four different empirical fit models, namely the Band function, the smoothly broken power law (SBPL), the cutoff power law (COMP) and the simple power law (PL). Among all fitted spectra, we further selected the "BEST"

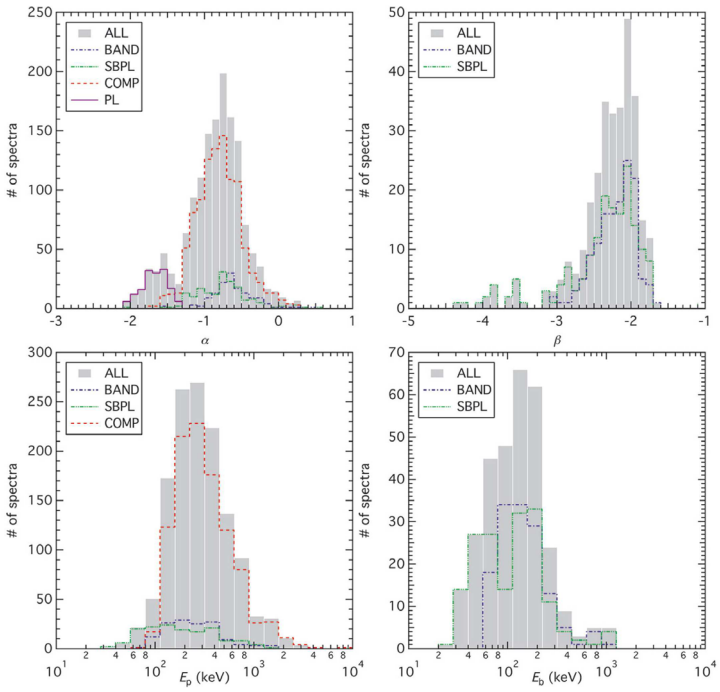


**Figure 3.** Distributions of the BEST sample spectral parameters: the low-energy spectral index $\alpha$, the high-energy spectral index $\beta$, the peak photon energy $E_p$ and the break energy $E_b$.

model sample adopting following criteria: that the relative error $\sigma_Q/Q \leq 0.4$ for each parameter $Q$ of a model and that $\sigma_\alpha \leq 0.4$ and $\sigma_\beta \leq 1.0$ for models that have two PL indices. 1491 spectra satisfy these criteria, and the distributions of the BEST sample spectral parameters are shown in Figure 3.

### 2.1 Discussion of the main results

We can summarize the main results of the time-resolved spectral analysis as follows. **(1)** The preferred model (in 69% of cases) is the COMP one. A possible reason might be a bias due to poor count statistics at high energies. However, GRBs in the LAT FoV which remain undetected show that upper limits are usually inconsistent with the GBM fit Band function's $\beta$, extrapolated to the LAT energy range. This might indicate a real manifestation of GRB physics. **(2)** There are no significant deviations of the distributions of fit parameters from those observed in the Fermi GBM GRB time-integrated spectral catalogs. The comparison of averaged time-resolved parameters to time-integrated ones shows that averaged time-resolved $\alpha$ and $E_p$ are harder than time-integrated ones. **(3)** We observed the widening of time-integrated spectra with respect to the time-resolved ones (see also [7, 8]). This effect might be caused by the time-integrated analysis, and this might lead to incorrect physical interpretations. **(4)** We performed a search for plausible blackbody components in time-resolved spectra, adding simulations on individual bursts. Unfortunately, only three GRBs out of the whole sample show extra blackbody components in multiple time bins.

### Acknowledgments

The GBM project is supported by NASA. Support for the German contribution to GBM was provided by the *Bundesministerium für Bildung und Forschung* via the *Deutsches Zentrum für Luft und Raumfahrt* under contract number 50 QV 0301. E.B. is supported by the Italian *Fondo di Sviluppo e Coesione 2007-2013 - APQ Ricerca Regione Puglia "Future In Research"*.

## References

[1] P. N. Bhat et al., The Astrophysical Journal Supplement Series **223-2** 28 (2016)
[2] H.-F. Yu et al., Astronomy & Astrophysics **588** A135 (2016)
[3] V. Connaughton et al., The Astrophysical Journal Supplement Series **216-2**, 32 (2015)
[4] A. Hoover et al., Il Nuovo Cimento C **28**, 797-800 (2005)
[5] C. Fraley & A. E. Raftery, J. Am. Stat. Assoc. **97** 611 (2000)
[6] S. J. Gershman & D. M. Blei, Journal of Math. Psychology **56** 1 (2012)
[7] H.-F. Yu et al., Astronomy & Astrophysics **583** A129 (2015)
[8] M. Axelsson & L. Borgonovo, Monthly Notices of the Royal Astron. Society **447** 3150 (2015)